Alisporivir Normalizes Mitochondrial Function of Primary Mouse Lung Endothelial Cells Under Conditions of Hyperglycemia

Vlada S. Starinets[1,2], Dmitriy A. Serov[3,4], Nikita V. Penkov[4], Natalia V. Belosludtseva[1,2], Mikhail V. Dubinin[1], and Konstantin N. Belosludtsev[1,2,a]*

[1]Mari State University, 424001 Yoshkar-Ola, Mari El, Russia
[2]Institute of Theoretical and Experimental Biophysics, Russian Academy of Sciences, 142290 Pushchino, Moscow Region, Russia
[3]Biophotonics Center, Prokhorov General Physics Institute, Russian Academy of Sciences, 119991 Moscow, Russia
[4]Institute of Cell Biophysics, Russian Academy of Sciences, 142290 Pushchino, Moscow Region, Russia
[a]e-mail: bekonik@gmail.com

Abstract—Effect of alisporivir (a mitochondrial permeability transition pore inhibitor) on the development of mitochondrial dysfunction under hyperglycemic conditions in the primary culture of mouse lung endothelial cells was investigated in this work. We demonstrated that hyperglycemia (30 mM glucose for 24 h) leads to the decrease in viability of the pulmonary endotheliocytes, causes mitochondrial dysfunction manifested by the drop in membrane potential and increase in superoxide anion generation as well as facilitates opening of the mitochondrial permeability transition pore (MPT pore). Incubation of endothelial cells with 5 µM alisporivir under hyperglycemic conditions leads to the increase in cell viability, restoration of the membrane potential level and of the MPT pore opening activity to control values. Hyperglycemia causes increased mitophagy in the lung endothelial cells: we observed increase in the degree of colocalization of mitochondria and lysosomes and upregulation of the *Parkin* gene expression. Alisporivir restores these parameters back to the levels observed in the control cells. Hyperglycemia results in the increase in the expression of the *Drp1* gene in endotheliocytes responsible for synthesis of the protein involved in the process of mitochondria fission. Alisporivir does not significantly alter expression of the genes. The paper discusses mechanisms of the effect of alisporivir on mitochondrial dysfunction in murine pulmonary endotheliocytes under conditions of hyperglycemia.

DOI: 10.1134/S0006297922070033

Keywords: mitochondria, alisporivir, mitochondrial permeability transition pore, hyperglycemia, diabetes mellitus, mitophagy

INTRODUCTION

Diabetes mellitus is a metabolic disease caused either by inadequate secretion of insulin by pancreatic β cells (type I diabetes mellitus) or by insulin resistance of the human and animal organs and tissues (type II diabetes mellitus). In both cases this leads to the development of hyperglycemia, accompanied by dysregulation of protein and lipid metabolism. These disorders lead to pathological changes in the organs and tissues of the body [1-5].

Mitochondrial dysfunction is generally recognized as one of the processes involved in the development of diabetes mellitus at the cellular level [6, 7]. Indeed, for many organs and tissues, as well as cell lines, it has been demonstrated that diabetes mellitus or hyperglycemia lead to the increased generation of reactive oxygen species by mitochondria, disruption of oxidative phosphorylation processes, and drop of the membrane potential. It is believed that this is due to dysregulation of the cellular quality control of mitochondria, intracellular system responsible for mitophagy, mitochondrial biogenesis, and mitochondrial dynamics [6-9].

Opening of the Ca^{2+}-dependent pore (mitochondrial permeability transition pore, MPT pore) in the inner mitochondrial membrane is one of the important signs of mitochondrial dysfunction [10, 11]. The MPT pore is

---

* To whom correspondence should be addressed.

considered to be a protein mega-channel formed in the inner and outer membranes of mitochondria in the presence of excessive concentration of Ca^{2+}, development of oxidative stress, and under effect of a number of other modulators. Under conditions of maximum penetrability, this channel is permeable for compounds with molecular weight up to 1500 Da, which causes collapse of the membrane potential, disruption of ion homeostasis, swelling of organelles, and their destruction [12-14]. Despite the fact that the mitochondrial pore has been studied for more than 50 years, its structure and mechanism of formation are still far from being resolved. The only reliably established protein involved in the MPT pore induction is mitochondrial matrix cyclophilin D. Cyclophilin D is considered as a regulator of the MPT pore, and inhibitors of this protein (cyclosporine A, alisporivir) suppress opening of the MPT pore at submicromolar concentrations [10-16]. At present, adenine nucleotide translocator and ATP synthase are considered as hypothetical MPT pore proteins in the inner membrane [14].

Analysis of the literature data suggests that the development of diabetes mellitus is accompanied by the tissue-specific changes in the sensitivity of mitochondria to MPT pore induction [6]. In particular, a number of organs and tissues (skeletal muscles, heart, pancreas) show increase in the sensitivity of mitochondria to the factors triggering opening of the MPT pore during the development of diabetes mellitus [6, 17-19]. At the same time, liver mitochondria become more resistant to MPT pore opening [20, 21]. Possibly, this also explains why the pharmacological and genetic modulation of MPT pore does not always lead to the development of a therapeutic effect. In particular, on the one hand, knockout of cyclophilin D or its inhibition did not affect the development of diabetic nephropathy [22]. On the other hand, mice lacking cyclophilin D under conditions of high-fat diet showed the ability to increase glucose uptake by the skeletal muscle cells [23], and MPT pore inhibitors were able to reduce the size of the infarct zone in the diabetic animals during ischemia/reperfusion [6, 24]. In the previous studies, we have shown that the long-term (3 weeks) administration of the MPT pore inhibitor alisporivir (a non-immunosuppressive analogue of cyclosporine A) to the mice with induced diabetes leads to alleviation of the effects of diabetic mitochondrial dysfunction in the skeletal and cardiac muscles. Moreover, alisporivir increases the rate of glucose utilization from the blood of diabetic animals during the glucose tolerance test [25, 26]. In the present work, we continue to study the effect of alisporivir on mitochondrial dysfunction induced by hyperglycemia. Research at the cellular level often reveals molecular and intracellular mechanisms that cannot be observed *in vivo* in animal experiments. The objectives of this study were: (i) to determine the effect of alisporivir on viability of the primary culture of mouse lung endothelial cells in hyperglycemia; (ii) to evaluate the effect of alisporivir on hyperglycemia-induced mitochondrial dysfunction of pulmonary endotheliocytes; (iii) to determine the effect of alisporivir on colocalization of mitochondria and lysosomes in the pulmonary endothelial cells under conditions of hyperglycemia, thereby determining possible effect of this agent on mitophagy; (iv) to determine the level of expression of genes encoding proteins responsible for mitochondrial biogenesis, mitophagy, and mitochondrial dynamics in the lung endotheliocytes under conditions of hyperglycemia in the absence and presence of alisporivir.

MATERIALS AND METHODS

Isolation and culturing of mouse endothelial cells. Endothelial cells were isolated from mouse lung microvessels by indirect magnetic separation [27, 28]. BALB/c mice (male, weight 20-22 g) were used in the work. Animals were euthanized by cervical dislocation. Under sterile conditions, lungs were removed from the chest, washed in DMEM (Gibco, USA), and minced with surgical scissors. After grinding, the tissue sample was incubated in 0.2% collagenase type II solution (Abcam, UK) for 40 min at 37°C and constant stirring. The samples were resuspended and passed through a sieve with a pore diameter of 70 μm (Greiner Bio-One, Austria). A 20%-serum was added to the cell suspension and then centrifuged twice at 500*g* for 8 min. Cells were resuspended in a phosphate-buffered saline without calcium and magnesium salts and supplemented with 2 mM EDTA and antibodies against CD31 (Abcam) (1 : 100 dilution) followed by incubation for 15 min with constant stirring, washed by centrifugation at 500*g* for 8 min. After washing, the cells were incubated for 15 min with magnetic particles conjugated with the secondary antibodies (1 : 100 dilution) (Thermo Fisher, USA). Separation of $CD31^+$ cells was performed with a MagJET magnetic rack (Thermo Fisher). Cells were washed five times with phosphate buffered saline and seeded into culture flasks with bottom pretreated with a solution of 0.2% gelatin from bovine skin (Sigma-Aldrich, USA). The resulting cells were cultured according to the standard protocol in a DMEM : F12 medium (1 : 1) supplemented with 10% fetal bovine serum, 2 mM L-glutamine, 100 U/ml penicillin, 100 μg/ml streptomycin, and 25 μg/ml amphotericin B (all from Gibco) and 50 μg/ml endothelial cell growth supplement (Sigma-Aldrich). The culture was obtained by combining cells from three animals [27]. Cells of passage 7-10 with viability estimated by propidium iodide staining of at least 98% were used in the experiments. Round coverslips (25 mm diameter) were placed one at a time into the wells of 6-well plates. A solution of 0.2% gelatin was applied to coverslips, dried, and next a suspension of endothelial cells in the culture medium was added. The cells were cultured for 3 days until confluence

level of 90% or more was reached.

Modeling of hyperglycemia. Hyperglycemia was modeled by cell incubation in a culture medium with an elevated glucose concentration of 30 mM for 24 h in a CO_2 incubator (Sanyo, Japan) [29]. Control cells were incubated for 24 h in a culture medium with a glucose concentration of 5 mM. Half of the samples were incubated with 5 µM alisporivir. Alisporivir (Medchemexpress, Monmouth Junction, USA, cat. no. HY-12559) was added to the culture medium as a solution in DMSO (1 : 2000 dilution), cells without alisporivir were incubated for 24 h after addition of the appropriate volume of DMSO.

Assessment of cell viability. To assess cell viability, immediately after the end of incubation cells were washed three times with Hank's solution (PanEco, Russia) and incubated for 30 min with 5 µg/ml of Hoechst 33342 vital dye and 5 µM propidium iodide (both from Thermo Fisher) at 37°C. Fluorescence of the cells was recorded using a LED imaging system based on an AE31E inverted microscope (Motic, Spain) equipped with a Motic PLAN FLU-AR 10× N.A. 0.3 objective [30]. Image analysis was performed using the Image J2 (Fiji) software (NIH, USA).

Determination of the mitochondrial membrane potential in endotheliocytes. A fluorescent dye rhodamine 123 (Thermo Fisher) was used to determine potential on the inner mitochondrial membrane. Immediately after the end of incubation, the cells were washed three times with Hank's solution and stained with rhodamine 123 (excitation wavelength 485 nm, emission wavelength 525 nm) at concentration of 2.5 µg/ml for 30 min at 37°C. Next, the cells were washed three times with Hank's solution. Cell fluorescence was recorded using the LED imaging system described above. All measurements were performed at constant excitation light source current (80 mA), exposure time (1 s), gain (×623), and pixel averaging (2×2). Fluorescence intensity of rhodamine 123 was expressed as the ratio of fluorescence intensity at each point (F) to average fluorescence intensity under basic conditions (F_0). To assess the membrane potential, 2 µM FCCP was added and change in the fluorescence intensity was determined. For the convenience of comparing data between the samples, the membrane potential was expressed as a percentage. Change in the fluorescence intensity in the control cells was taken as 100%.

Determination of colocalization of mitochondria and lysosomes in endotheliocytes. Colocalization of mitochondria and lysosomes in endotheliocytes was assessed using confocal microscopy based on colocalization of fluorescent dyes MitoTracker DeepRed FM (200 nM) and LysoTracker Green (50 nM) (both from Thermo Fisher) in the cells [31]. Confocal images were obtained using a DMI6000 microscope (Leica, Germany). A 488 nm argon laser was used to excite LysoTracker Green fluorescence, and emission was measured at 505-530 nm. Fluorescence of MitoTracker DeepRed was excited at 638 nm with a Ne/He laser. Fluorescence was measured at 650-680 nm. Colocalization analysis was performed using the Image J2 (Fiji) software (NIH, USA). Proportion of the area of colocalization of mitochondria and lysosomes was calculated as a fraction of the total area of mitochondria in the field of view (taken as 100%). For each sample, at least 10 fields of view were analyzed. For each experimental condition, four biological replicates were performed (coverslip with cells of a separate culture).

Determination of mitochondrial pore opening in endotheliocytes. Mitochondrial pore induction was assessed using a calcein-AM fluorescence in the presence of 1 mM $CoCl_2$ [32, 33]. After incubation with the studied agents, the cells from four experimental groups were washed three times with Hank's solution and incubated for 30 min at 37°C in the presence of 1 µM calcein-AM, 200 nM MitoTracker Red (for visualization of the mitochondrial structure), and 1 mM $CoCl_2$. After staining, the cells were washed with Hank's balanced salt solution and fluorescence images were acquired using a DMI6000 confocal microscope (Leica). Mitochondria were identified using MitoTracker DeepRed fluorescence and intensity of the calcein-AM fluorescence (excitation wavelength 494 nm, emission wavelength 517 nm) in them was measured. Image analysis was performed using the Image J2 (Fiji) software (NIH, USA). Background fluorescence intensity was subtracted from the cell fluorescence intensity. Fluorescence intensity of calcein-AM was calculated relative to fluorescence intensity of MitoTracker. For each experimental condition, four biological repetitions were performed (two coverslips with cells of a separate culture).

Assessment of oxidative stress in endotheliocytes. The level of oxidative stress was assessed by flow cytometry using a Muse Cell Analyzer (Luminex, USA). For flow cytometry, endothelial cells of each group were detached from the substrate using a solution containing trypsin (0.05%) and EDTA (0.53 mM) for 10 min at 37°C. The detached cells were transferred into 5 ml of DMEM medium with 10% fetal bovine serum to inhibit trypsin, mixed, and centrifuged at 350g for 8 min, the pellet was resuspended in 100 µl of sterile Hank's solution. Glucose was added to hyperglycemic cells to a concentration of 30 mM. Quantification of the cell population exposed to oxidative stress was assessed using a Muse Oxidative Stress Kit (MCH100111) (Luminex). All experiments were performed strictly according to the manufacturer's protocol.

ROS production was also assessed using a fluorescent dye 2',7'-dichlorodihydrofluorescein diacetate (H_2DCFDA) (Thermo Fisher). Cells of the four experimental groups were stained with 20 µM H_2DCFDA for 30 min at 37°C. Next, the cells were washed with Hank's solution and analyzed using a LED imaging system at 490 nm excitation and 520 nm emission wavelengths.

Quantitative real-time PCR. The level of expression of genes encoding proteins responsible for mitophagy, mi-

List of gene-specific primers for RT-PCR analysis

Gene	Forward (5'→3')	Reverse (5'→3')
Drp1	TTACAGCACACAGGAATTGT	TTGTCACGGGCAACCTTTTA
Mfn2	CACGCTGATGCAGACGGAGAA	ATCCCAGCGGTTGTTCAGG
Ppargc1a	CTGCCATTGTTAAGACCGAG	GTGTGAGGAGGGTCATCGTT
Pink1	TTGCCCCACACCCTAACATC	GCAGGGTACAGGGGTAGTTCT
Parkin	AGCCAGAGGTCCAGCAGTTA	GAGGGTTGCTTGTTTGCAGG
Rplp2	CGGCTCAACAAGGTCATCAGTGA	AGCAGAAACAGCCACAGCCCCAC

tochondrial biogenesis, and mitochondrial dynamics was determined using real-time reverse transcription PCR (RT-PCR) [26]. Total RNA was obtained from cell suspension samples using an ExtractRNA reagent (Evrogen, Russia) according to the manufacturer's protocol. Real-time PCR was performed using a QuantStudio 1 amplifier (Thermo Fisher) with a qPCRmix-HS SYBR kit (Evrogen), where SYBR Green II was used as a fluorescent intercalating dye. Selection and analysis of the gene-specific primers was performed using Primer-BLAST [34] (the sequence of oligonucleotides is presented in table). The *Rplp2* mRNA level was used to normalize expression of each gene. Calculation of ΔΔCt was carried out according to the formula ΔΔCt = ΔCt (Control) − ΔCt (experiment); each ΔCt value was calculated using the formula ΔCt = Ct (tested gene) − Ct (Rplp2) [35].

Statistical data processing. GraphPad Prism version 7.0 for Windows (GraphPad Software Inc., USA) was used for statistical data analysis. One-way ANOVA, followed by Tukey's *post hoc* test, was used to assess statistical significance of differences between groups. The results were presented as mean ± standard deviation ($n = 4$-6, where n is the number of experiments with different cultures).

RESULTS

Alisporivir increases viability of the mouse lung endotheliocytes under hyperglycemia. Viability of the cells in the primary culture of mouse pulmonary endothelial cells maintained under conditions of normo- (5 mM) and hyperglycemia (30 mM) and in the absence and presence of 5 μM alisporivir is shown in Fig. 1 and Fig. S1 in the Online Resource 1. This concentration of alisporivir was chosen based on a series of preliminary experiments on isolated mitochondria (data not shown). One can see that incubation of cells for 24 h under hyperglycemic conditions resulted in the significant reduction in the number of live cells. Presence of alisporivir in the incubation medium led to the increase in viability of the mouse lung endotheliocytes under conditions of hyperglycemia.

Alisporivir suppresses development of mitochondrial dysfunction in the mouse lung endotheliocytes under hyperglycemia. In the previous studies, we have shown that *in vivo* administration of alisporivir to the mice with type II diabetes normalizes functioning of heart and skeletal muscle mitochondria [25, 26]. In this work, we evaluated the effect of alisporivir on mitochondria functioning in the primary culture of mouse lung endotheliocytes un-
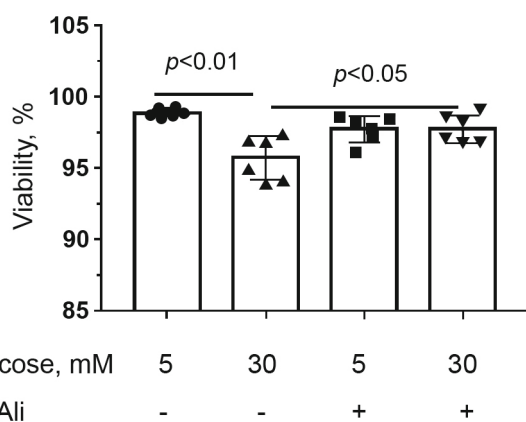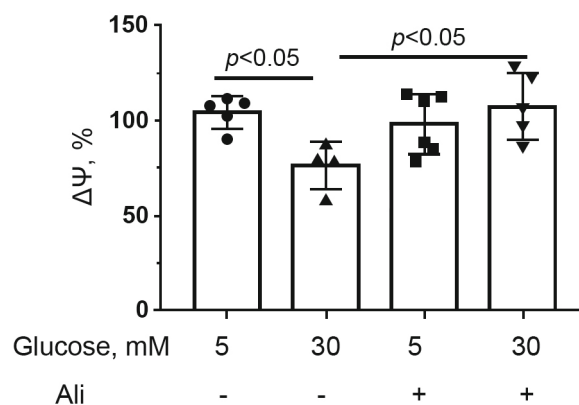

Fig. 1. Effect of alisporivir (Ali, 5 μM) on survival of the mouse lung endothelial cells under conditions of normo- (5 mM glucose) and hyperglycemia (30 mM glucose). The data are presented as mean ± SD ($n = 6$).

Fig. 2. Effect of alisporivir (Ali, 5 μM) on ΔΨ (%) of mitochondria of the mouse lung endotheliocytes under conditions of normo- (5 mM glucose) and hyperglycemia (30 mM glucose). The data are presented as mean ± SD ($n = 4$).
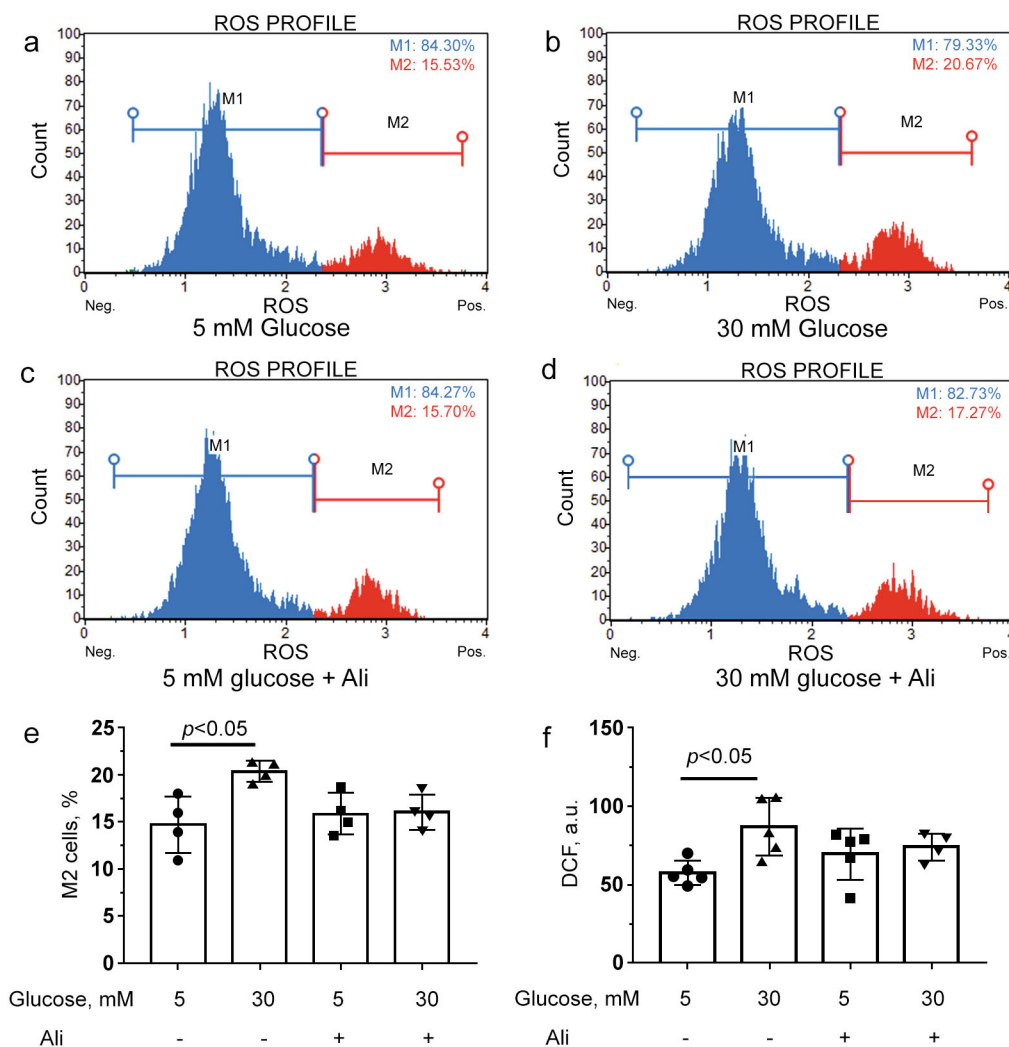
Fig. 3. Effect of alisporivir (Ali, 5 μM) (c and d) on production of reactive oxygen species by the pulmonary endotheliocytes under conditions of normo- (5 mM glucose) (a and c) and hyperglycemia (30 mM glucose) (b and d). a-d) Typical distribution diagrams of the cell population in four experimental groups. e) Calculation of ROS-positive cells (%) in the experimental groups. f) Level of DCF fluorescence in the cells of four experimental groups. The data are presented as mean ± SD (n = 4-5).

der conditions of hyperglycemia. Figure 2 shows that the endotheliocytes incubated in the medium with high concentration of glucose (30 mM) had a reduced membrane potential (ΔΨ) compared to the control cells (5 mM glucose). Incubation of the cells with 5 μM alisporivir under hyperglycemic conditions resulted in normalization of the mitochondrial membrane potential to control level (Fig. S2 in the Online Resource 1).

In parallel with mitochondrial depolarization, oxidative stress develops under conditions of hyperglycemia. Typical flow cytometry data reflecting the number of ROS-positive and ROS-negative cells in each group are shown in Fig. 3, a-d. One can see that under the used conditions, there is an increase in the number of ROS-positive cells (population of the cells with superoxide-induced fluorescence related to the M2 peak) indicating increased generation of superoxide anions in endotheliocytes. In the presence of alisporivir, we did not find a significant

decrease in the number of ROS-positive cells under conditions of hyperglycemia, although a downward trend was observed (Fig. 3e). Similar results were obtained by fluorescence microscopy using the DCF probe (Fig. 3f and Fig. S3 in the Online Resource 1).

Alisporivir is an MPT pore inhibitor [15]. In this regard, in the next part of the work, we determined its effect on the opening of the MPT pore in the cells of the primary culture of mouse lung endothelial cells exposed to hyperglycemia. The MPT pore activity in the mitochondria of endotheliocytes was assessed from fluorescence of calcein in mitochondria in the presence of cobalt ions. In the case of disruption of the integrity of mitochondrial membrane, including formation of the MPT pore, $CoCl_2$ penetrates into mitochondria and causes quenching of the calcein fluorescence. Thus, decrease in the intensity of calcein fluorescence in mitochondria indicates opening of the MPT pore. Figure 4 shows typical pulmonary endothe-
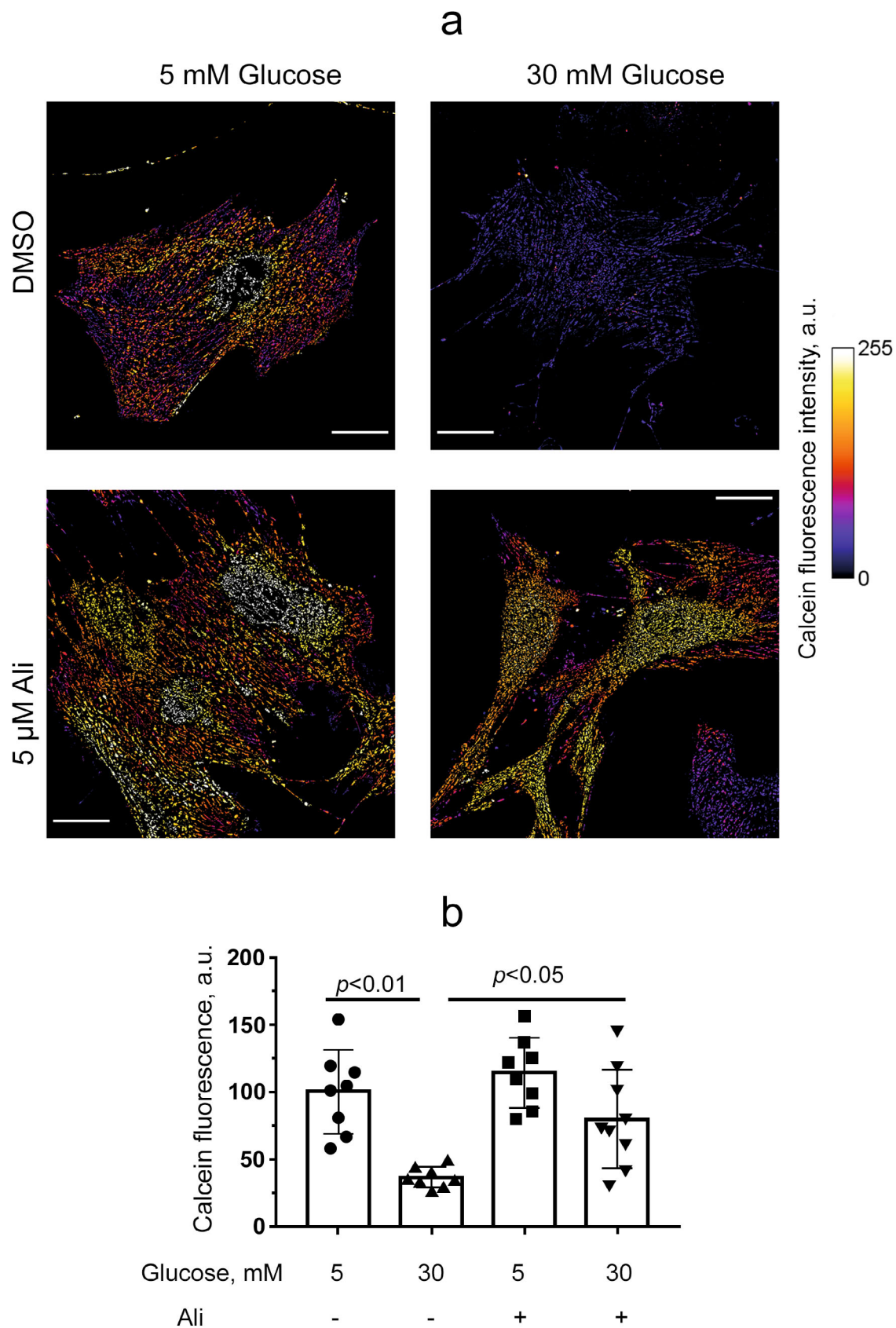
a

Fig. 4. MPT pore induction in the mouse lung endotheliocytes. a) typical images of mitochondrial calcein fluorescence in the presence of $CoCl_2$ in the endothelial cells of the experimental groups. Scale bar − 40 μm. b) Intensity of calcein fluorescence in mitochondria of the mouse lung endotheliocytes from four experimental groups. The data are presented as mean ± SD ($n = 4$).
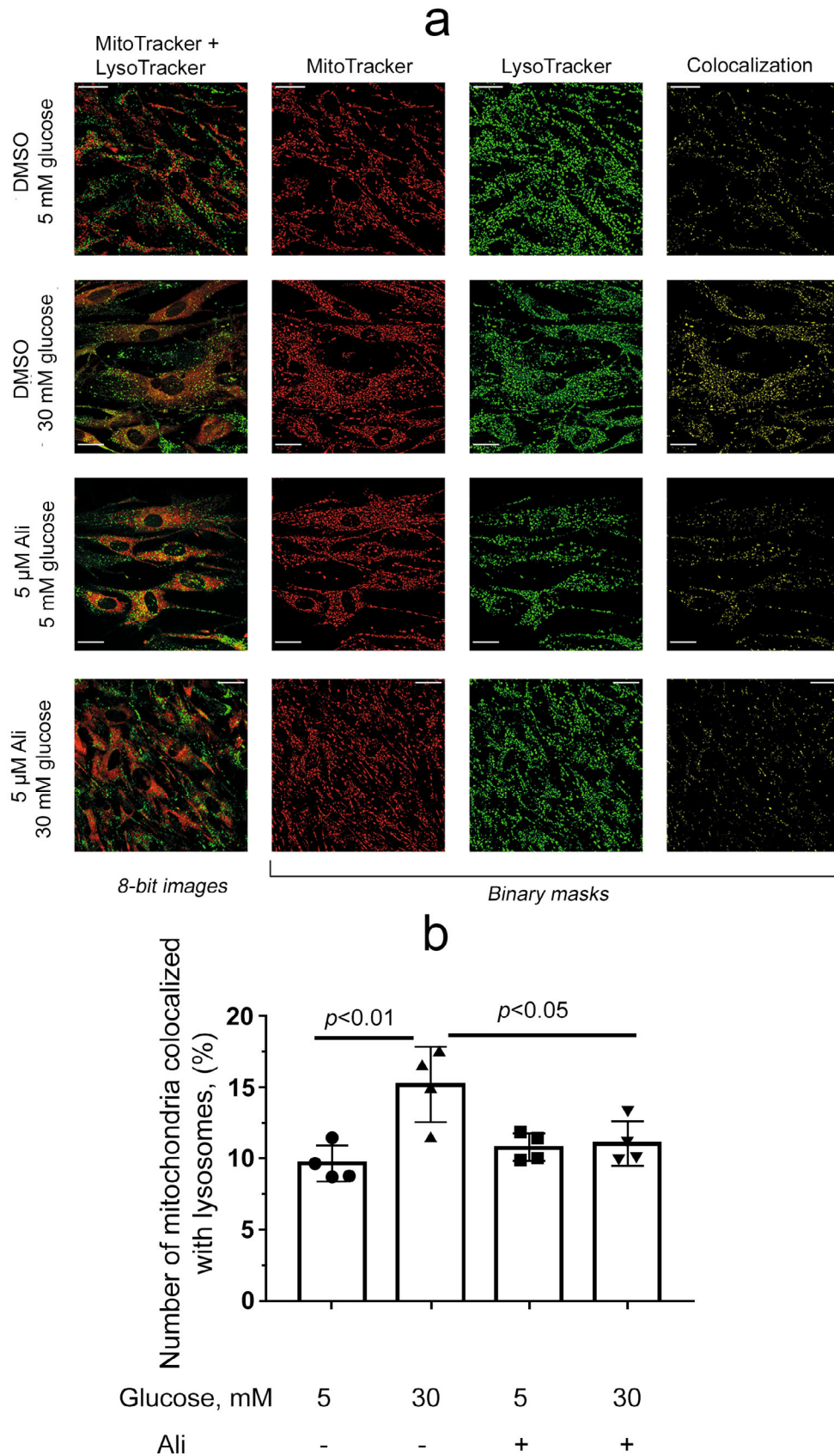
Fig. 5. Colocalization of mitochondria and lysosomes in the mouse lung endotheliocytes from four experimental groups. Colocalization of mitochondria and lysosomes was determined by double staining of cells using MitoTracker DeepRed FM and LysoTracker Green. a) 8-bit images and binary masks of each dye and their colocalization are shown. b) Number of mitochondria (%) colocalized with lysosomes in the mouse lung endotheliocytes from four experimental groups. The data are presented as mean ± SD ($n = 4$).

liocytes under four experimental conditions stained with calcein in the presence of cobalt ions. It should be noted that the MPT pore can be in both a high- and a low-conductance states [12]. Cobalt ions can penetrate into the mitochondrial matrix in both states. Thus, one could assume that the fluorescence quenching observed in the control cells is associated with the spontaneous low-conductance state of the MPT pore. It can be seen that the mitochondria of endotheliocytes under conditions of elevated glucose content show a significant decrease in the intensity of calcein fluorescence compared to the control cells (Fig. 4). This suggests that hyperglycemia increases the MPT pore opening activity in endotheliocytes.

Incubation of the cells with alisporivir under conditions of hyperglycemia leads to the significant increase in the intensity of calcein fluorescence in mitochondria compared to the mitochondria of endotheliocytes incubated only in the presence of 30 mM glucose (Fig. 4). This suggests that alisporivir inhibits opening of the MPT pore in the inner mitochondrial membrane of endotheliocytes exposed to hyperglycemia. We also calculated proportion of the mitochondria not stained with calcein: in the control experiment, the content of such mitochondria was $9.5 \pm 2.1\%$. Under the conditions of hyperglycemia, proportion of such mitochondria increased significantly to $23.2 \pm 6.6\%$. In the presence of alisporivir, we observed a trend towards decrease in the number of mitochondria not stained with calcein to $17.6 \pm 6.2\%$. This also confirms that hyperglycemia stimulates opening of the MPT pore in endotheliocytes, and alisporivir interferes with this effect.

Alisporivir inhibits hyperglycemia-induced colocalization of mitochondria and lysosomes (mitophagy). Mitophagy (mitochondrial autophagy) is one of the adaptive responses to hyperglycemia and reduced membrane potential in mitochondria [6, 36]. In this work, we assessed the level of mitophagy by the degree of colocalization of mitochondria and lysosomes using the double cell staining method (MitoTracker DeepRed FM and LysoTracker Green). We have found that under conditions of 24 h hyperglycemia, the degree of colocalization of mitochondria and lysosomes significantly increases, which may indicate increase in mitophagy. Under these conditions, incubation of the mouse lung endotheliocytes with 5 µM alisporivir led to normalization of the level of colocalization of mitochondria and lysosomes to control values (Fig. 5).

Effect of alisporivir on changes in the level of mRNA of proteins responsible for mitochondrial biogenesis, mitochondrial dynamics, and mitophagy under conditions of hyperglycemia. In the next part of the work, we evaluated expression of the genes encoding proteins responsible for mitochondrial biogenesis, mitophagy, and mitochondrial dynamics. It was found that hyperglycemia is associated with the significant increase in the level of *Drp1* expression, which may indirectly indicate increase in the amount of Drp1 protein involved in the processes of mi-

tochondrial fission (Fig. 6). Incubation of the cells with 5 µM alisporivir under hyperglycemic conditions did not lead to the significant changes in the expression of this gene, although there was a trend towards restoration of the control values. In all the studied groups, there were no significant differences in the expression of the *Ppargc1a* gene responsible for the synthesis of PGC1a, a protein involved in mitochondrial biogenesis, and of the *Mfn2* gene responsible for the synthesis of mitofusin 2, a protein involved in the process of mitochondrial fusion. It should be noted that hyperglycemic conditions are associated with the significant increase in the expression of *Parkin* (but not *Pink1*), which is responsible for the synthesis of a protein involved in mitophagy. This indirectly confirms the data obtained in the previous part of the work demonstrating that hyperglycemia (30 mM glucose for 24 h) induces mitophagy in the mouse lung endotheliocytes. Addition of 5 µM alisporivir to the cells exposed to 30 mM glucose resulted in the significant decrease in *Parkin* expression to the control level.

DISCUSSION

Mitochondrial dysfunction is one of the main manifestations of the development of diabetes mellitus [6]. A number of studies have shown that the mitochondria-targeted gene or pharmacological therapy restores structural and functional parameters of mitochondria, reduces complications of diabetes mellitus, including increase in the insulin sensitivity of tissues and organs, and has a hypoglycemic effect [23, 25, 37]. In the previous studies, we have shown that the long-term treatment of diabetic mice with alisporivir (an MPT pore inhibitor) leads to both decrease in the mitochondrial dysfunction in skeletal and cardiac muscles and increase in the rate of glucose utilization from the blood during a glucose tolerance test [25]. In the present work, we examined intracellular mechanisms that may underlie the protective effect of alisporivir against the high glucose-mediated damage in the mouse lung endotheliocytes.

We have demonstrated that the exposure of pulmonary endotheliocytes to hyperglycemic conditions led to the development of mitochondrial dysfunction, manifested by the increased generation of reactive oxygen species, MPT pore induction, and mitochondrial depolarization, as a consequence of these factors (Figs. 2-5). These dysfunctions of mitochondria may underlie the cell death. Indeed, we observed decrease in viability of the pulmonary endotheliocytes under conditions of hyperglycemia (Fig. 1). Incubation of the cells with alisporivir (5 µM) under hyperglycemic conditions largely eliminates the development of signs of mitochondrial dysfunction. We have found that there is a decrease in the number of MPT perforated mitochondria in endotheliocytes and, consequently, normalization of the transmembrane potential of
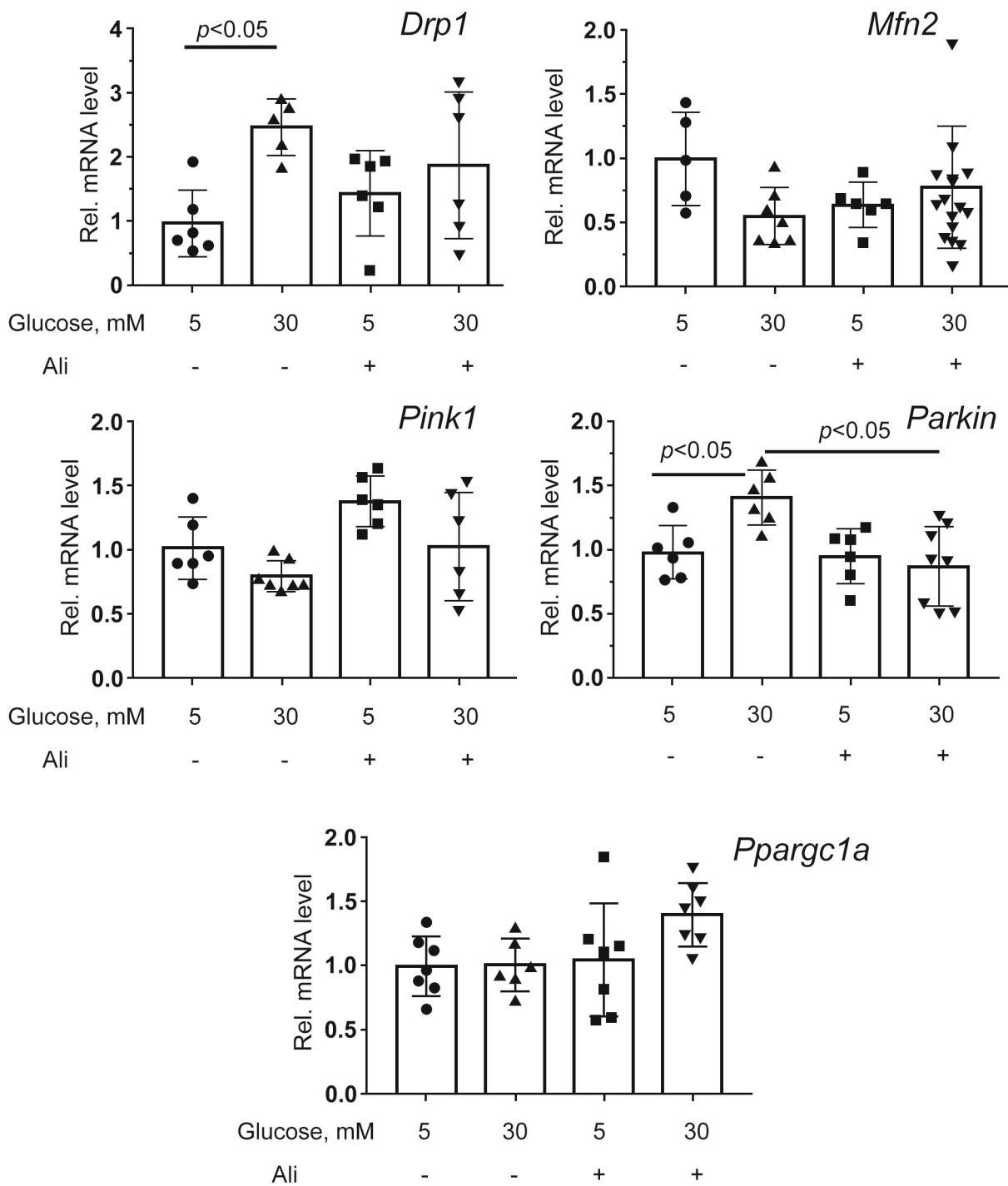
Fig. 6. Relative levels of *Drp1*, *Mfn2*, *Pink1*, *Parkin*, and *Ppargc1a* mRNAs in the mouse lung endotheliocytes from four experimental groups. The data are presented as mean ± SD ($n = 6$).

mitochondria, which becomes comparable with the mitochondrial potential of the control cells. Decrease in the production of reactive oxygen species in the cells under hyperglycemic conditions in the presence of alisporivir was not observed (only a trend towards decrease in the production of ROS compared to the hyperglycemic conditions was noted). Nevertheless, the alisporivir-induced

normalization of mitochondrial functions described above led to the increase in the number of surviving cells under conditions of hyperglycemia.

Decrease in the transmembrane potential in mitochondria is considered to be one of the factors initiating mitophagy [31, 38]. In our experiments under conditions of hyperglycemia and reduced membrane potential, we

observed increase in colocalization of mitochondria and lysosomes and increase in the expression of the gene encoding Parkin protein involved in mitophagy in endotheliocytes. It is important to note that these methodological approaches are indirect evidence of mitophagy. However, they suggest activation of this protein under conditions of hyperglycemia, which is in agreement with the literature data. It is known that the stage of prediabetes is associated with activation of mitophagy, while the stage of type II diabetes mellitus is associated with inhibition of this process [6, 39]. In this case, activation of mitophagy is considered as an adaptive response. Apparently, exposure of the primary culture of mouse endothelial cells for 24 h to the medium containing 30 mM glucose causes decrease in the cell viability and development of mitochondrial dysfunction. However, the cells can alternatively activate processes (in particular, mitophagy) that prevent this negative scenario.

Incubation of the cells under conditions of hyperglycemia with alisporivir led to the level of colocalization of mitochondria and lysosomes, as well as the level of *Parkin* gene expression being indistinguishable from those observed in the control cells. Thus, one could assume that under hyperglycemic conditions, alisporivir not only prevents formation of the MPT pore and decrease in the mitochondrial membrane potential, but also, possibly, inhibits initiation of mitophagy in endotheliocytes. Further studies evaluating mitophagy are needed to prove this assumption.

One could debate whether the lack of adaptive response such as mitophagy is beneficial during the development of diabetes mellitus, but our previous studies suggest that alisporivir has a therapeutic effect during long-term administration to diabetic animals [25, 26]. Indeed, we have previously demonstrated that the heart of diabetic mice exhibits decrease in the expression of the *Pink1* and *Parkin* genes, and long-term (3 weeks) administration of alisporivir to diabetic animals leads to normalization of the expression of these genes [26].

As shown in this work, in addition to the changes in the *Parkin* gene expression, hyperglycemia causes increase in the content of mRNA of the Drp1 protein responsible for mitochondrial fission. These results indirectly confirm the data available in the literature that the development of diabetes mellitus in humans and animals, as well as in the hyperglycemia cell models is accompanied by fragmentation of the mitochondrial network [6-8]. Under our conditions, alisporivir could not reliably restore the level of *Drp1* mRNA to control values.

As mentioned above, studies at the cellular level make it possible to identify mechanisms and target molecules that cannot be detected in animal experiments. Alisporivir, like its immunosuppressive analog cyclosporin A, has several targets [40, 41]. In addition to the mitochondrial cyclophilin D, alisporivir is able to interact with cytoplasmic cyclophilin A [41]. This action is associated with its ability to suppress replication of various viruses in cells, including SARS-CoV-2 [42]. Therefore, the effects obtained in this work may be due not only to the action of this agent on mitochondria. However, it is clear that alisporivir, both in *in vivo* experiments in animals and in experiments with cell culture, suppresses development of mitochondrial dysfunction in diabetes mellitus and contributes to alleviation of the course of this disease.

Ethics declarations. The authors declare no conflicts of interest in financial or any other sphere. All applicable international, national, and/or institutional guidelines for the care and use of animals were followed.

Electronic supplementary material. The online version contains supplementary material available at https://doi.org/10.1134/S0006297922070033.

REFERENCES

1. American Diabetes Association Professional Practice Committee (2022) 2. Classification and Diagnosis of Diabetes: Standards of Medical Care in Diabetes-2022, *Diab. Care*, **45 (Suppl 1)**, S17-S38, doi: 10.2337/dc22-S002.

2. DeFronzo, R. A., Ferrannini, E., Groop, L., Henry, R. R., Herman, W. H., et al. (2015) Type 2 diabetes mellitus, *Nat. Rev. Dis. Primers*, **1**, 15019, doi: 10.1038/nrdp.2015.19.

3. Skyler, J. S., Bakris, G. L., Bonifacio, E., Darsow, T., Eckel, R. H., et al. (2017) Differentiation of diabetes by pathophysiology, natural history, and prognosis, *Diabetes*, **66**, 241-255, doi: 10.2337/db16-0806.

4. Roden, M., and Shulman, G. I. (2019) The integrative biology of type 2 diabetes, *Nature*, **576**, 51-60, doi: 10.1038/s41586-019-1797-8.

5. Nolan, C.J., Prentki, M. (2019) Insulin resistance and insulin hypersecretion in the metabolic syndrome and type 2 diabetes: Time for a conceptual framework shift, *Diab. Vasc. Dis. Res.*, **16**, 118-127, doi: 10.1177/1479164119827611.

6. Belosludtsev, K. N., Belosludtseva, N. V., Dubinin, M. V. (2020) Diabetes mellitus, mitochondrial dysfunction and Ca^{2+}-dependent permeability transition pore, *Int. J. Mol. Sci.*, **21**, 6559, doi: 10.3390/ijms21186559.

7. Montgomery, M. K., and Turner, N. (2015) Mitochondrial dysfunction and insulin resistance: An update, *Endocr. Connect.*, **4**, R1-R15, doi: 10.1530/EC-14-0092.

8. Fujimaki, S., and Kuwabara, T. (2017) Diabetes-induced dysfunction of mitochondria and stem cells in skeletal

muscle and the nervous system, *Int. J. Mol. Sci.*, **18**, E2147, doi: 10.3390/ijms18102147.

9. Dai, W., Lu, H., Chen, Y., Yang, D., Sun, L., and He, L. (2021) The loss of mitochondrial quality control in diabetic kidney disease, *Front Cell Dev Biol.*, **9**, 706832, doi: 10.3389/fcell.2021.706832.

10. Belosludtsev, K. N., Dubinin, M. V., Belosludtseva, N. V., and Mironova, G. D. (2019) Mitochondrial Ca^{2+} transport: mechanisms, molecular structures, and role in cells, *Biochemistry* (*Moscow)*, **84**, 593-607, doi: 10.1134/S0006297919060026.

11. Bonora, M., Patergnani, S., Ramaccini, D., Morciano, G., Pedriali, G., et al. (2020) Physiopathology of the permeability transition pore: molecular mechanisms in human pathology, *Biomolecules*, **10**, 998, doi: 10.3390/biom10070998.

12. Neginskaya, M. A., Pavlov, E. V., and Sheu, S. S. (2021) Electrophysiological properties of the mitochondrial permeability transition pores: Channel diversity and disease implication, *Biochim. Biophys. Acta. Bioenerg.*, **1862**, 148357, doi: 10.1016/j.bbabio.2020.148357.

13. Zoratti, M., and Szabo, I. (1995) The mitochondrial permeability transition, *Biochim. Biophys. Acta*, **1241**, 139-176, doi: 10.1016/0304-4157(95)00003-a.

14. Bernardi, P., Carraro, M., and Lippe, G. (2021) The mitochondrial permeability transition: Recent progress and open questions, *FEBS J.*, doi: 10.1111/febs.16254.

15. Šileikytė, J., and Forte, M. (2016) Shutting down the pore: The search for small molecule inhibitors of the mitochondrial permeability transition, *Biochim Biophys Acta*, **1857**, 1197-1202, doi: 10.1016/j.bbabio.2016.02.016.

16. Efimov, S. V., Dubinin, M. V., Kobchikova, P. P., Zgadzay, Y. O., Khodov, I. A., et al. (2020) Comparison of cyclosporin variants B-E based on their structural properties and activity in mitochondrial membranes, *Biochem. Biophys. Res. Commun.*, **526**, 1054-1060, doi: 10.1016/j.bbrc.2020.03.184.

17. Oliveira, P. J., Seiça, R., Coxito, P. M., Rolo, A. P., Palmeira, C. M., et al. (2003) Enhanced permeability transition explains the reduced calcium uptake in cardiac mitochondria from streptozotocin-induced diabetic rats, *FEBS Lett.*, **554**, 511-514, doi: 10.1016/s0014-5793(03)01233-x.

18. Lablanche, S., Cottet-Rousselle, C., Lamarche, F., Benhamou, P. Y., Halimi, S., et al. (2011) Protection of pancreatic INS-1 β-cells from glucose- and fructose-induced cell death by inhibiting mitochondrial permeability transition with cyclosporin A or metformin, *Cell Death Dis.*, **2**, e134, doi: 10.1038/cddis.2011.15.

19. Monaco, C., Hughes, M. C., Ramos, S. V., Varah, N. E., Lamberz, C., et al. (2018) Altered mitochondrial bioenergetics and ultrastructure in the skeletal muscle of young adults with type 1 diabetes, *Diabetologia*, **61**, 1411-1423, doi: 10.1007/s00125-018-4602-6.

20. Ferreira, F. M., Seiça, R., Oliveira, P. J., Coxito, P. M., Moreno, A. J., et al. (2003) Diabetes induces metabolic adaptations in rat liver mitochondria: Role of coenzyme Q and cardiolipin contents, *Biochim. Biophys. Acta*, **1639**, 113-120, doi: 10.1016/j.bbadis.2003.08.001.

21. Belosludtsev, K. N., Starinets, V. S., Belosludtsev, M. N., Mikheeva, I. B., Dubinin, M. V., et al. (2021) Chronic treatment with dapagliflozin protects against mitochondrial dysfunction in the liver of C57BL/6NCrl mice with high-fat diet/streptozotocin-induced diabetes mellitus, *Mitochondrion*, **59**, 246-254, doi: 10.1016/j.mito.2021.06.008.

22. Lindblom, R., Higgins, G. C., Nguyen, T. V., Arnstein, M., Henstridge, D. C., et al. (2020) Delineating a role for the mitochondrial permeability transition pore in diabetic kidney disease by targeting cyclophilin D, *Clin. Sci.*, **134**, 239-259, doi: 10.1042/CS20190787.

23. Taddeo, E. P., Laker, R. C., Breen, D. S., Akhtar, Y. N., Kenwood, B. M., et al. (2013) Opening of the mitochondrial permeability transition pore links mitochondrial dysfunction to insulin resistance in skeletal muscle, *Mol. Metab.*, **3**, 124-134, doi: 10.1016/j.molmet.2013.11.003.

24. Najafi, M., Farajnia, S., Mohammadi, M., Badalzadeh, R., Ahmadi Asl, N., et al. (2014) Inhibition of mitochondrial permeability transition pore restores the cardioprotection by postconditioning in diabetic hearts, *J. Diabetes Metab. Disord.*, **13**, 106, doi: 10.1186/s40200-014-0106-1.

25. Belosludtsev, K. N., Starinets, V. S., Talanov, E. Y., Mikheeva, I. B., Dubinin, M. V., et al. (2021) Alisporivir treatment alleviates mitochondrial dysfunction in the skeletal muscles of C57BL/6NCrl mice with high-fat diet/streptozotocin-induced diabetes mellitus, *Int. J. Mol. Sci.*, **22**, 9524, doi: 10.3390/ijms22179524.

26. Belosludtseva, N. V., Starinets, V. S., Mikheeva, I. B., Serov, D. A., Astashev, M. E., et al. (2021) Effect of the MPT pore inhibitor alisporivir on the development of mitochondrial dysfunction in the heart tissue of diabetic mice, *Biology (Basel)*, **10**, 839, doi: 10.3390/biology10090839.

27. Sobczak, M., Dargatz, J., and Chrzanowska-Wodnicka, M. (2010) Isolation and culture of pulmonary endothelial cells from neonatal mice, *J. Vis. Exp.*, **46**, e2316, doi: 10.3791/231.

28. Serov, D. A., Tankanag, A. V., and Astashev, M. E. (2022) Low frequency oscillations of murine skin microcirculations and periodic changes of $[Ca^{2+}]_i$ and $[NO]_i$ levels in murine endotheliocytes: an effect of provocative tests, *Cell Biol. Int.*, **46**, 427-442, doi: 10.1002/cbin.11743.

29. Lee, W. C., Chau, Y. Y., Ng, H. Y., Chen, C. H., Wang, P. W., et al. (2019) Empagliflozin protects HK-2 cells from high glucose-mediated injuries via a mitochondrial mechanism, *Cells*, **8**, 1085, doi: 10.3390/cells8091085.

30. Serov, D., Tikhonova, I., Safronova, V., and Astashev, M. (2021) Calcium activity in response to nAChR ligands in murine bone marrow granulocytes with different Gr-1 expression, *Cell Biol. Int.*, **45**, 1533-1545, doi: 10.1002/cbin.11593.

31. Berezhnov, A. V., Soutar, M. P., Fedotova, E. I., Frolova, M. S., Plun-Favreau, H., et al. (2016) Intracellular pH modulates autophagy and mitophagy, *J. Biol Chem.*, **291**, 8701-8708, doi: 10.1074/jbc.M115.691774.

32. Sasaki, K., Donthamsetty, R., Heldak, M., Cho, Y. E., Scott, B. T., et al. (2012) VDAC: old protein with new roles in diabetes, *Am. J. Physiol. Cell Physiol.*, **303**, 1055-1060, doi: 10.1152/ajpcell.00087.2012.

33. Zhao, Z., Gordan, R., Wen, H., Fefelova, N., Zang, W. J., et al. (2013) Modulation of intracellular calcium waves and triggered activities by mitochondrial Ca flux in mouse cardiomyocytes, *PLoS One*, **8**, e80574, doi: 10.1371/journal.pone.0080574.

34. Ye, J., Coulouris, G., Zaretskaya, I., Cutcutache, I., Rozen, S., et al. (2012) Primer-BLAST: A tool to design target-specific primers for polymerase chain reaction, *BMC Bioinformatics*, **13**, 134, doi: 10.1186/1471-2105-13-134.

35. Schmittgen, T. D., and Livak, K. J. (2008) Analyzing real-time PCR data by the comparative C(T) method, *Nat. Protoc.*, **3**, 1101-1108, doi: 10.1038/nprot.2008.73.

36. Onphachanh, X., Lee, H. J., Lim, J. R., Jung, Y. H., Kim, J. S., et al. (2017) Enhancement of high glucose-induced PINK1 expression by melatonin stimulates neuronal cell survival: Involvement of MT_2/Akt/NF-$\varkappa$B pathway, *J. Pineal Res.*, **63**, e12427, doi: 10.1111/jpi.12427.

37. Benton, C. R., Holloway, G. P., Han, X. X., Yoshida, Y., Snook, L. A., et al. (2010) Increased levels of peroxisome proliferator-activated receptor gamma, coactivator 1 alpha (PGC-1alpha) improve lipid utilisation, insulin signalling and glucose transport in skeletal muscle of lean and insulin-resistant obese Zucker rats, *Diabetologia*, **53**, 2008-2019, doi: 10.1007/s00125-010-1773-1.

38. Narendra, D., Tanaka, A., Suen, D. F., and Youle, R. J. (2008) Parkin is recruited selectively to impaired mitochondria and promotes their autophagy, *J. Cell Biol.*, **183**, 795-803, doi: 10.1083/jcb.200809125.

39. Bhansali, S., Bhansali, A., Walia, R., Saikia, U. N., and Dhawan, V. (2017) Alterations in mitochondrial oxidative stress and mitophagy in subjects with prediabetes and type 2 diabetes mellitus, *Front. Endocrinol.*, **8**, 347, doi: 10.3389/fendo.2017.00347.

40. Dubinin, M. V., Sharapov, V. A., Ilzorkina, A. I., Efimov, S. V., Klochkov, V. V., et al. (2022) Comparison of structural properties of cyclosporin A and its analogue alisporivir and their effects on mitochondrial bioenergetics and membrane behavior, *Biochim. Biophys. Acta. Biomembr.*, **1864**, 183972, doi: 10.1016/j.bbamem.2022.183972.

41. Di Lisa, F., Carpi, A., Giorgio, V., and Bernardi, P. (2011) The mitochondrial permeability transition pore and cyclophilin D in cardioprotection, *Biochim. Biophys. Acta*, **1813**, 1316-1322, doi: 10.1016/j.bbamcr.2011.01.031.

42. Softic, L., Brillet, R., Berry, F., Ahnou, N., Nevers, Q., et al. (2020) Inhibition of SARS-CoV-2 infection by the cyclophilin inhibitor Alisporivir (Debio 025), *Antimicrob. Agents Chemother.*, **64**, e00876-20, doi: 10.1128/AAC.00876-20.